Confocal Microscopy Study of Texture Transitions in a Polymer Stabilized Cholesteric Liquid Crystal

G. A. Held,[1] L. L. Kosbar,[1] I. Dierking,[1,]* A. C. Lowe,[1] G. Grinstein,[1] V. Lee,[2] and R. D. Miller[2]
[1]*IBM T. J. Watson Research Center, P.O. Box 218, Yorktown Heights, New York 10598*
[2]*IBM Almaden Research Center, 650 Harry Road, San Jose, California 95120*

(Received 7 May 1997)

The switching transition of polymer stabilized cholesteric texture liquid crystals is studied via confocal microscopy. This noninvasive probe enables the simultaneous imaging of the polymer network and the liquid crystal domain structure. We find that the two-stage switching often occurring in these systems results from the cholesteric experiencing two distinct environments: one consisting of very low polymer density, and the other strongly dominated by the polymer network. Fluctuations in the local polymer density produce effective random fields that broaden the transition. [S0031-9007(97)04319-6]

PACS numbers: 61.30.Gd, 61.41.+e, 64.70.Md, 85.60.Pg

The use of polymer networks to stabilize and modify liquid crystal phases for display-based applications has recently become widespread [1]. Reverse mode polymer stabilized cholesteric textures (PSCTs) represent one such class of polymer stabilized liquid crystals—a class whose applicability extends to both reflective and transmissive displays [2,3]. In a reverse mode PSCT, a cholesteric [4,5] with a pitch of several microns (infrared) is situated between glass plates. The axis of the cholesteric helix is perpendicular to the plates, a configuration referred to as the planar state. A low concentration (typically 2%–10% by weight) of a reactive mesogenic monomer is dissolved in the liquid crystal. The monomer is then photopolymerized while the cholesteric is in the planar state. The helical structure of the cholesteric should thus be reflected in the resulting polymer network. In the absence of an applied electric field, this planar state is transparent to visible light. Application of a moderate electric field along the helical axis switches the system into the so-called "focal-conic" state, which scatters light strongly. In the switching process, the polymer network serves two important functions: First, it influences the structure of the focal-conic state, and thus greatly influences the scattering properties of the system, and, second, following the removal of the electric field, elastic forces between the polymer network and the liquid crystal cause the reorientation back to the planar texture to occur about 1000 times faster than in the absence of polymer. Such rapid switching is obviously desirable in display applications.

Much work has been done modifying the processing conditions of PSCTs so as to optimize their reflectivity. There is still, however, little understanding of the effect of the polymer on the switching process, or of the microscopic structure of the liquid crystal in the disordered, scattering (focal-conic) state. This state is often visualized as a multidomain structure with each domain defined by the orientation of the local helical axis of the cholesteric [3]. However, there have been no experimental observations in PSCTs which directly support this picture. The greatest impediment to the study of the switching transition has been the lack of a suitable probe: The optical anisotropy of the liquid crystal prevents light scattering studies, and the resolution of conventional optical microscopy is insufficient. While scanning electron microscopy does provide the necessary resolution, its use requires removing the liquid crystal and destroying the cell, so *in situ* imaging of either the switching process or the polymer network has not been possible.

We show here how confocal microscopy overcomes these limitations. This technique enables us to probe the switching transition *in situ* with a resolution of 0.2 μm. By tagging the polymer with a fluorophore, moreover, we are able simultaneously to resolve both the polymer network and the domain structure of the liquid crystal as the applied field is varied. We thereby produce the first *in situ* experimental verification of the polymer network following the helical orientation of the planar cholesteric liquid crystal. By observing that, as the field is increased, focal conic domains first form in regions of the sample with particularly low polymer concentration, we are also able to explain the two-stage switching transition previously observed [6] in systems with either sufficiently low polymer concentrations or a sufficiently coarse network. Finally, we argue that features of the observed switching are generally consistent with a simple random-field model, wherein local density fluctuations of the polymer network broaden the transition.

The liquid crystal material used for this study was an induced cholesteric consisting of the nematic mixture E48 (Merck Industries) and a chiral dopant, R1011 (Merck). The dopant concentration was chosen to produce a cholesteric pitch of 10 μm. Two different reactive monomers were studied: RM206 (Merck), a mesogenic diacrylate, and BMBB-6, a mesogenic dimethacrylate [3]. A monomer mixture—composed of 93% monomer, 2% photoinitiator, and 5% of a monofunctional fluorescent tag molecule (pyrene-1-butanol methacrylate)—was dissolved in the chiral nematic liquid crystal, with concentrations of 4% and 6% by weight.

The liquid crystal/monomer solutions were vacuum filled into cells of 15 μm gap with rubbed polyimide alignment layers, which induce ordering of the adjacent liquid crystal molecules parallel to the rubbing direction, thus promoting the formation of the planar state. The cells were specially constructed; one wall was made of indium-tin oxide (ITO) coated glass, while the other was made from an ITO coated, 0.17 mm thick cover slip, so as to allow study with a high resolution oil immersion lens. The cells were sealed and irradiated with a UV source (0.5 mW/cm^2) for 5.5 h to induce polymerization, while the liquid crystal remained in the planar orientation. The resulting polymer network structure is thus expected to follow the local helical order of the liquid crystal. Incorporation of the fluorescent taggant into the polymer network permitted fluorescent imaging of the network.

The micrographs presented below were collected with a Zeiss LSM 410 confocal microscope operating in reflective geometry [7]. Light from a 488 nm Ar laser is focused to a small spot within the sample. As this spot is rastered across the sample with a mirror, an image is constructed from the reflected light, which is detected with a photomultiplier. A pinhole, located directly in front of the detector, serves as a spatial filter; it ensures that only focused light (i.e., light from the focal plane within the sample) enters the detector. It is this pinhole which provides the depth resolution of the microscope—it ensures that the illumination, specimen, and detector all have the same focus (that is, are confocal). Using a 63X oil immersion objective lens, together with a 20 μm pinhole, we obtained a spatial resolution of approximately 0.2 μm.

When a 515 nm low pass filter is placed in front of the detector, only fluorescence resulting from the 488 nm illumination is detected, whereupon the polymer network (the only component of the cell that fluoresces) is imaged. Similar fluorescence confocal microscopy techniques have recently been used to study polymer morphology within polymer dispersed liquid crystals [8]. When the low pass filter is replaced by a polarizer oriented at 90° to the polarization of the incident laser beam, depolarized scattered light (488 nm) is collected. This results in imaging of the disordered regions within the liquid crystal (i.e., those no longer in the planar cholesteric texture). Switching between the low pass filter and the polarizer enables us to image either the polymer network or the liquid crystal texture at exactly the same position within the cell.

Figures 1(a)–1(c) show confocal micrographs of a 4% RM206 PSCT cell taken at depths of 4, 5, and 6 μm below the upper liquid crystal-polyimide boundary. These images were taken with fluorescence detection, so the bright parts of the image show the polymer network. The presence of dark regions in these micrographs indicates that there is complete phase separation between polymer and liquid crystal. If polymerization were not complete, and fluorescent monomers remained dissolved in the liquid crystal, these dark regions would fluoresce as well. It is also clear from these figures that the polymer network reflects the helical order of the liquid crystal in which it was polymerized: The polymer strands are oriented in a well-defined direction within each plane, and this direction rotates by 35° between planes separated by 1 μm—corresponding quite precisely to the 10 μm pitch of the cholesteric material. Helical order, albeit less pronounced, is also present (but not shown here), for the 6% BMBB-6 PSCTs. In this case, large liquid crystal filled voids are also present in the network [cf. Fig. 3(d) below], in agreement with scanning electron microscopy (SEM) data [3,6].

The diffuse reflectivity of 6% BMBB-6, 4% RM206, and 6% RM206 PSCT cells as a function of applied voltage is plotted in Figs. 2(a)–2(c). These reflectivities were measured on an absolute scale with an integrating sphere and a 633 nm HeNe laser, using methods presented elsewhere [6]. The two stages of the switching between the planar and focal-conic states are most clearly observable for the 6% BMBB-6 data. They are present, although less obvious, in the 4% RM206 data. The switching of the 6% RM206 sample, however, occurs in a single stage.

Figures 3(a)–3(c) are confocal images of the 6% BMBB-6 sample, taken with polarizing detection at applied fields of 8, 10.5, and 13.5 V. Figure 3(d) is a fluorescence detection confocal image of the polymer network in the same region, taken with no applied field. At 8 V [Fig. 3(a)] the onset of a focal-conic domain is readily observable. At 10.5 V the focal-conic domain (seen as the darkened region of the micrograph) has grown to approximately 20 μm in diameter; domains of this size cover about one-quarter of the sample. As the voltage across the cell is further increased, these domains multiply, expand, and, at approximately 13.5 V, form a structure which extends across the entire sample [Fig. 3(c)]. The arrows in Fig. 2(a) allow one to correlate these three portraits of domain development with the behavior of the diffuse reflectivity. The earliest formation of focal-conic domains (at 8 V) corresponds to the onset of the initial steep ("first stage") rise of the reflectivity. The growth of localized domains corresponds to a point (10.5 V) midway through this first stage of the increase in reflectivity, and the formation of the extended domain network shown in Fig. 3(c) occurs at the beginning of second-stage increase.

The effect of the polymer network on the switching properties of the PSCT cell can be understood by comparing the observed evolution of domains within the liquid crystal [Figs. 3(a)–3(c)] with the polymer network in the same region in space [Fig. 3(d)]. The initial nucleation of the focal-conic domain occurs in a void in the polymer network, that is, in a region of pure liquid crystal. The larger domain of Fig. 3(b) is centered around voids and generally occupies a region of lower than average polymer density.

To understand the observed switching behavior, consider first the case of a planar cholesteric in the absence of any polymer. As the voltage across the cell is

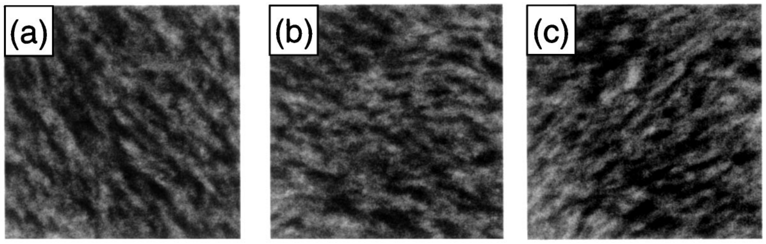

FIG. 1. (a)–(c) Fluorescence detection confocal micrographs of the polymer network within a 4% RM206 PSCT cell, taken at depths of 4, 5, and 6 μm, respectively. The length of each image is 25 μm.

increased, the liquid crystal undergoes a sharp transition from the planar state to a fingerprint texture, which is a series of domains with helical axes aligned *perpendicular* to the applied field [4]. As the voltage is increased further, the helices unwind and the liquid crystal becomes "homeotropic," i.e., all of the rodlike molecules become oriented in the direction (say z) of the applied field.

Since the polymer network in the PSCT follows the helical pattern of the planar state, it produces a field conjugate to the helical order parameter of this state. This field, which opposes the rotation of the helical axes into the fingerprint orientation, is strongest where the polymer density is highest. This picture can be formalized in a simple random-field model, wherein the standard elastic free energy [4] for a cholesteric in an electric field is supplemented by a phenomenological random-field term of the form $U \int s(\vec{r})\,[\hat{h}(z)\cdot\vec{n}(\vec{r})]^2\,d\vec{r}$. Here $s(\vec{r})$ is 1 or 0 for, respectively, positions $\vec{r}$ occupied or unoccupied by a polymer molecule; U is the polymer-liquid crystal interaction strength; $\hat{h}(z)$ is a unit vector in the plane of the glass plates, whose orientation follows the uniform rotation of the ideal planar texture; and $\vec{n}(\vec{r})$ gives the orientation of the liquid crystal molecules at position $\vec{r}$.

Complete analysis of this model is difficult, but one can readily understand some of the qualitative features of the switching transition by estimating the free energy change associated with rotating the helical axis of a liquid crystal droplet of linear size l from the z direction into the xy plane. This free energy, $\Delta F(l)$, can be written as

$$\Delta F(l) \sim Jl - E^2 l^3 + UM(l)\,. \qquad (1)$$

The three terms represent, respectively, the elastic energy cost (of strength J) of rotating the droplet out of the otherwise planar configuration, the bulk field-energy gain in an applied field proportional to E, and the polymer-liquid crystal interaction energy cost. $M(l)$, the total volume of polymer in the droplet, is approximated as $M(l) \sim cl^3 \pm \sqrt{c(1-c)}\,l^{3/2}$; here the $l^{3/2}$ term crudely accounts for the standard square-root statistical fluctuations in the polymer density, the plus and minus signs

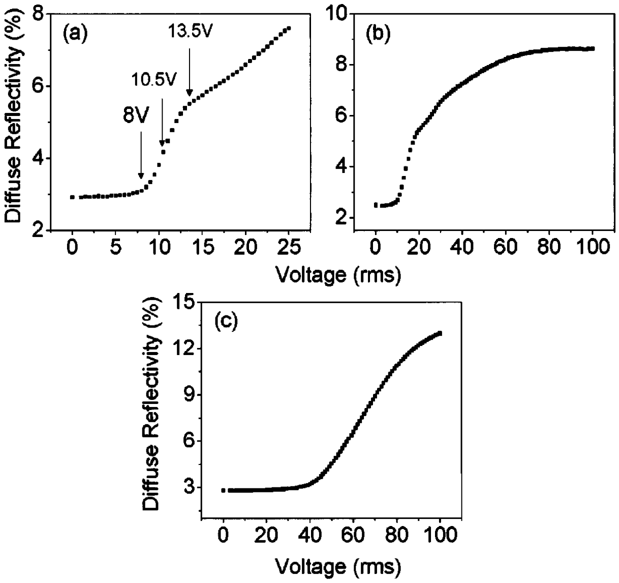

FIG. 2. Voltage dependence of the diffuse reflectivity for 15 μm thick PSCT cells with polymer concentrations of (a) 6% BMBB-6, (b) 4% RM206, and (c) 6% RM206. The applied voltages are rms values of a 2 kHz sine wave. The three arrows in (a) identify the voltages at which the images in Figs. 3(a)–3(c) were taken.

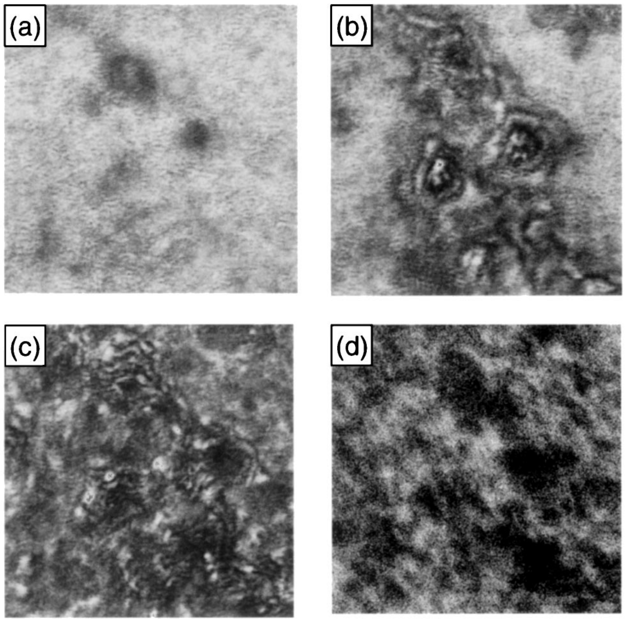

FIG. 3. (a)–(c) Polarized detection confocal micrographs of a 6% BMBB-6 PSCT cell, taken at applied potentials of 8, 10.5, and 13.5 V, respectively. Domains which have switched out of the planar texture appear as darkened regions. (d) Fluorescence detection confocal micrograph of the polymer network at the same region as (a)–(c), taken with no applied voltage. The length of each image is 25 μm.

corresponding, respectively, to droplets rich or deficient in polymer; c is the average fraction of liquid crystalline material in close enough proximity to the polymer to be influenced by it (which is somewhat different from the mean polymer concentration *per se*).

It is easy to see that for sufficiently small l, the free energy $\Delta F(l)$ is positive for any l, even for droplets deficient in polymer; thus it is energetically unfavorable to rotate any droplets. There is, however, a critical value of E, $E_{c1} \sim \sqrt{cU(1-\delta)}$, where $\delta \equiv 27c(1-c)^2 U^3/256J^3$, at which polymer-deficient droplets of size $l_{\min} = 16J^2/9c(1-c)U^2$ can lower their energy by rotating into the fingerprint alignment. It is simple to show from (1) that, as E increases above E_{c1}, droplets with l's in an expanding band around $l_{\min}$ likewise gain energy by rotating. At $E = E_c \equiv \sqrt{cU}$, polymer-deficient droplets of arbitrarily large size rotate. For $E > E_c$, therefore, only polymer-rich droplets remain unrotated. Such droplets are surrounded by liquid crystal already rotated into the fingerprint texture, so the elastic energy term Jl in Eq. (1) now *favors* rotation, i.e., acquires a negative sign. As E increases from E_c, the only polymer-rich droplets remaining unrotated are those in a steadily narrowing band of l's around $l_{\min}$. At $E = E_{c2} \equiv \sqrt{cU(1+\delta)}$, this band shrinks to zero, leaving everything rotated into the fingerprint texture.

This model predicts a broad, single-stage switching transition, as in Fig. 2(c); the two-stage switching of Figs. 2(a) and 2(b) results from the presence of large regions of anomalously low polymer density within the network [Fig. 3(d)]—regions for which our simple approximation to $M(l)$ does not account. Figures 3(a) and 3(d) make clear that for 6% BMBB-6, the switching begins in large voids. The liquid crystal in a void of linear size l_v has no polymer inhibiting its rotation, and so rotates when E exceeds the elastic term $\sqrt{Jl_v^{-2}}$. If this value of E is less than E_{c1} of our droplet approximation, then liquid crystal in the voids will rotate into the fingerprint texture first, initiating the transition. The first "stage" of the transition is produced by the spreading of these rotated domains over a larger region containing several voids [Fig. 3(b)]. For larger E, the first stage gives way to the broadened "second stage" transition described by our droplet model.

For the 4% RM206 sample, which has smaller fluctuations in polymer density (Fig. 1) than the 6% BMBB-6 sample [Fig. 3(d)], the first stage of the switching process appears to result from droplets of rotated liquid crystal forming in regions of anomalously low (but not zero) polymer density. These droplets are seen with confocal microscopy in a narrow voltage range; at higher fields they form a structure that spans the entire sample.

For the 6% RM206 sample, the fine polymer network permeates the cell so completely that voids cannot be resolved with confocal microscopy (although they are observable with SEM [6]). In this case, only a single stage is discernible [Fig. 2(c)], presumably because even the largest polymer-deficient regions are too small for any droplets to rotate until E exceeds E_{c1}. Cross-polarization confocal data in this case reveal only a uniform darkening of the image with increasing voltage.

Since neither the polymer-density fluctuations responsible for two-stage switching, nor the unwinding of the helices at large E was included in our derivation of E_{c1} and E_{c2}, these two field values cannot be precisely identified in the experimental data. The droplet model predictions are nonetheless qualitatively consistent with the trends observed in these data. In particular, since E_c, E_{c1}, and E_{c2} all increase with c, the model predicts that raising c will push the transition to higher applied fields. This is consistent with our 4% and 6% RM206 data—the 4% sample has a lower c and switches at lower fields. Further, SEM data show that RM206 networks are more finely stranded than BMBB-6 based ones [6]. Thus, for equal polymer content, an RM206 network will have greater liquid crystal/polymer interfacial area (resulting in a larger c) and will require a larger field to switch. This is in agreement with our 6% RM206 and 6% BMBB-6 data. Finally, the droplet model predicts that the "width" of the transition (approximated by $E_{c2} - E_{c1}$) should broaden with increasing c. This too is consistent with experimental observations [6].

We thank K. Plavetic and R. Moosher for assistance in sample preparation and confocal microscopy, respectively. A portion of this work was supported by NSF Grant No. DMR 9400354.

---

*Present address: Department of Physics, Chalmers University of Technology, S-41296 Göteborg, Sweden.

[1] For a review, see *Liquid Crystals in Complex Geometries,* edited by G.P. Crawford and S. Žumer (Taylor and Francis, London, 1996); see also P.S. Drzaic, *Liquid Crystal Dispersions* (World Scientific, Singapore, 1995).

[2] R.A.M. Hikmet and B.H. Zerver, Mol. Cryst. Liq. Cryst. **200**, 197 (1991); Liq. Cryst. **12**, 319 (1992); see also *Liquid Crystals in Complex Geometries,* Ref. [1], Chap. 3.

[3] D.-K. Yang, L.-C. Chien, and J.W. Doane, Appl. Phys. Lett. **60**, 3102 (1992); see also *Liquid Crystals in Complex Geometries,* Ref. [1], Chap. 5.

[4] P.G. DeGennes and J. Prost, *The Physics of Liquid Crystals* (Clarendon Press, Oxford, 1993), 2nd ed.

[5] In cholesterics, the orientation of the long, rodlike liquid crystal molecules is constant in planes perpendicular to a well-defined axis, and rotates uniformly as one moves along that axis, producing a helical structure.

[6] I. Dierking, L.L. Kosbar, A.C. Lowe, and G.A. Held, J. Appl. Phys. **81**, 3007 (1997).

[7] For example, S.J. Wright *et al.,* Methods Cell Biol. **38**, 1 (1993).

[8] K. Amundson, A. van Blaaderen, and P. Wiltzius, Phys. Rev. E **55**, 1646 (1997).